

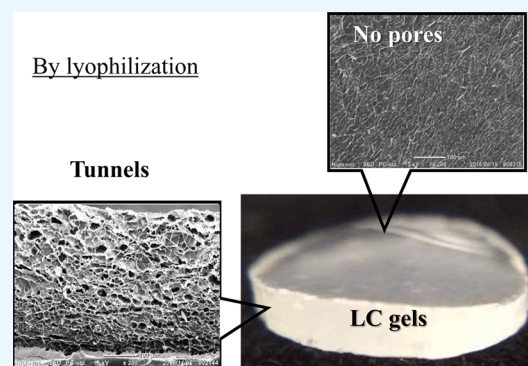
# Tough and Porous Hydrogels Prepared by Simple Lyophilization of LC Gels

Saranyoo Sornkamnerd,<sup>1</sup> Maiko K. Okajima, and Tatsuo Kaneko\*

Energy and Environment Area, School of Materials Science, Graduate School of Advanced Science and Technology, Japan Advanced Institute of Science and Technology (JAIST), 1-1 Asahidai, Nomi, Ishikawa 923-1292, Japan

## Supporting Information

**ABSTRACT:** Porous hydrogels possessing mechanical toughness were prepared from sacran, a supergiant liquid crystalline (LC) polysaccharide produced from *Aphanothece sacrum*. First, layered hydrogels were prepared by thermal cross-linking of film cast over a sacran LC solution. Then, anisotropic pores were constructed using a freeze-drying technique on the water-swollen layered hydrogels. Scanning electron microscopic observation revealed that pores were observable only on the side faces of sponge materials parallel to the layered structure but never on the top or bottom faces. The pore size, porosity, and swelling behavior were controlled by the thermal-cross-linking temperature. To clarify the freezing effect, a freeze–thawing method was used for comparison. The freeze–thawed hydrogels also formed layers but no pores. The mechanical properties and network structures of hydrogels were also studied, clarifying that porous hydrogels, even those with a high quantity of pores, were tough owing to the pores orienting along the layer direction like tunnels.



## INTRODUCTION

Porous hydrogels have been widely applied in the fields of artificial muscles, microfluidic valves, actuators, soft robotics, drug carriers, microlenses, supported catalysis, and chromatography.<sup>1–8</sup> Modulation of pore size and their distribution are essential for controlling hydrogel properties. Several strategies, such as gas foaming, fiber bonding, and porogen leaching, have been developed to fabricate hydrogels with homogeneous macropores for rapid stimuli response.<sup>2</sup> One of the simplest methods for forming pores in hydrogels is freeze drying and reswelling. The drawback of this method is that pore formation worsens the mechanical properties of the hydrogels, limiting their application.

Sacran is a newly developed sulfated polysaccharide extracted from a cyanobacterium, *Aphanothece sacrum*, which grows in underground freshwater. Sacran contains various sugar residues, such as Glc, Gal, Man, Xyl, Rha, Fuc, uronic acids, and muramic acids, where the chains are sulfated at a degree of 10–20 mol % to sugar residues (Figure S1). The sacran chain has a very high molecular weight of over  $2.0 \times 10^7$  g/mol (molecular length, over 30  $\mu\text{m}$ ) and shows self-assembly with increases in the solution concentration to achieve a rigid-rod structure at around 0.1%. In thicker solutions with concentrations ranging over 0.3%, the sacran solution exhibits a liquid crystalline (LC) phase.<sup>9</sup> Sacran has various properties, such as superhigh water-absorbing capacity, and has potential for wound-healing functions, anti-inflammatory effects, and antiallergic activities.<sup>10–12</sup> Another unique behavior of sacran is film formation with an in-plane orientation structure, which shows anisotropic

swelling. These properties of sacran and the above-mentioned importance of porous hydrogels motivated us to create tough and porous gels with molecular orientation of sacran LC chains.<sup>13,14</sup>

Here, we report a new, simple method of preparing layered sacran hydrogels with anisotropic pore structures by a casting and freeze-drying approach, although many other complicated methods have been reported for the preparation of porous hydrogels, such as metal–organic frameworks,<sup>15–17</sup> electrospinning,<sup>18–23</sup> gas foaming,<sup>24</sup> three-dimensional printing,<sup>25–28</sup> porogen leaching,<sup>29–31</sup> and freezing polymerization.<sup>32,33</sup> First, we used the conventional freeze-drying technique directly for sacran solution, but the resulting hydrogels were not self-standing presumably due to too high porosity. To impart toughness to porous hydrogels, we then freeze-dried the hydrogels in the water-swollen state instead of solution.

## RESULTS AND DISCUSSION

**Pore Formation in Hydrogels.** We made the porous sacran material using the freeze-drying technique, which is a conventional and simple method widely used for pore preparation in hydrogels.<sup>34</sup> The rationale was that sacran, having an ultrahigh molecular weight (>20 MDa) and a rigidity high enough to exhibit an LC phase, where sacran chains are intrinsically self-oriented in a very low concentration (>0.3 wt

Received: May 22, 2017

Accepted: July 21, 2017

Published: August 31, 2017

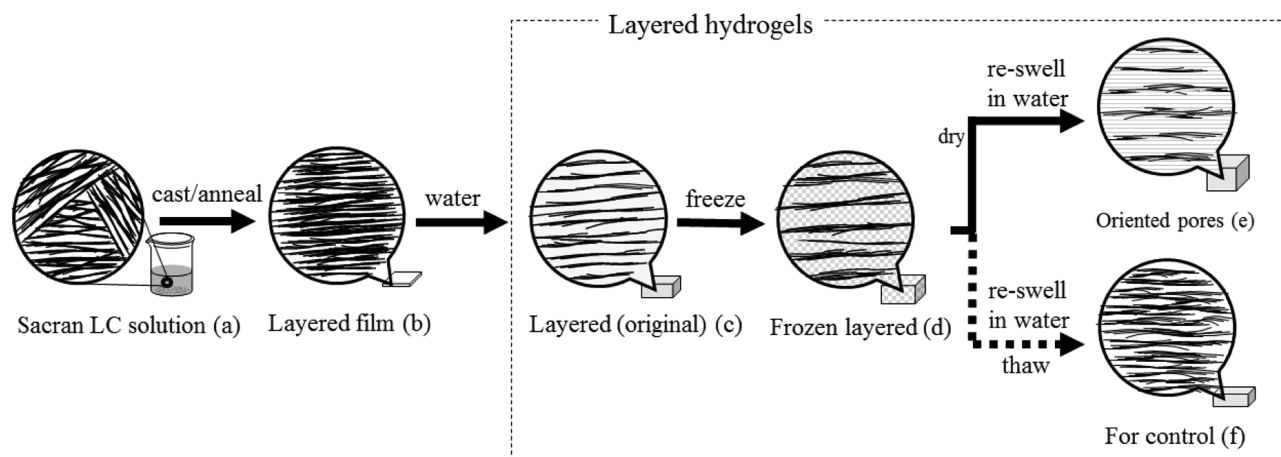


**Figure 1.** Schematic illustration of the preparation process for hydrogels with a layered structure and oriented pores. (a) Sacran LC solution with a concentration of 0.5% w/v. (b) Film with layered structures, where sacran chains were oriented in-plane, formed by casting of (a). (c) Hydrogels having a layered structure formed by water immersion of (b) after thermal cross-linking at various temperatures, which are basis of subsequently produced layered hydrogels. (d) Frozen hydrogels keeping a layered structure of sacran chains surrounded by ice crystal. (e) Hydrogels having the layered structure and oriented pores formed by freeze drying and successive water immersion of (d). In (f), (d) was thawed and immersed in water to prepare nondried hydrogels for comparison to (e).

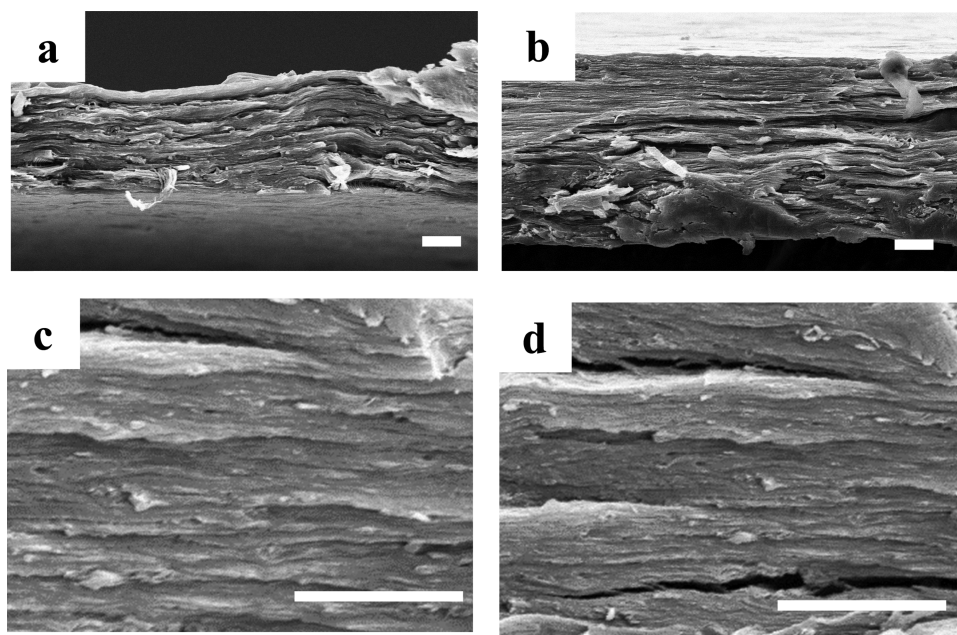


**Figure 2.** SEM images of cross-sectional sacran films cast from the LC solution and then thermally cross-linked at 60 °C (a, c) and 140 °C (b, d). Higher-magnification images (c, d) obviously revealed layered structures. The scale bar is 10  $\mu\text{m}$ .

%) as stated in [Introduction](#), might demonstrate the ability to form strong networks of hydrogels. First, the sacran solution was simply subjected to freeze drying to form spongy materials (representative picture, [Figure S2a](#)) and then the spongy sacran was annealed at 60 and 140 °C to examine the thermal-cross-linking behavior in the dried sponge state. Scanning electron microscopy (SEM) images of the sacran sponges were taken to observe the porous structure on their surfaces, as shown in [Figure S3a,b](#). The pore size of the sponges annealed at 60 °C was about  $6.0 \pm 1.5 \mu\text{m}$ , which is higher than those annealed at 140 °C ( $2.3 \pm 0.9 \mu\text{m}$ ). The pores created by freeze drying shrunk with successive annealing treatments, which suggested that the thermal cross-linking occurred due to the annealing treatment as demonstrated previously in the cast film test.<sup>35</sup> Besides, it has been reported in the literature that the

anisotropic structure of pores was controllable using freeze-drying technique.<sup>32</sup> The pore size is related to wettability of the substrate; hydrophobic substrate produced large pores, whereas the hydrophilic one produced tiny pores. The sponge annealed at 60 °C was immersed in deionized water for 24 h to turn it into a viscous solution but not into gels ([Figure S2b](#)), whereas the other at 140 °C created the intended gels after immersion in deionized water for 24 h ([Figure S2c](#)). These results indicated that the high annealing temperature is important for the gelation of the sacran sponges. The cross-linking junctions should be generated by not only heating but also freeze drying.<sup>33</sup> The swelling degree of the sacran sponges at 140 °C was  $57 \pm 6 \text{ g/g}$ , which is higher than that of nonporous hydrogels derived from sacran cast films due to the pores. As discussed previously, because sacran chains contain numerous

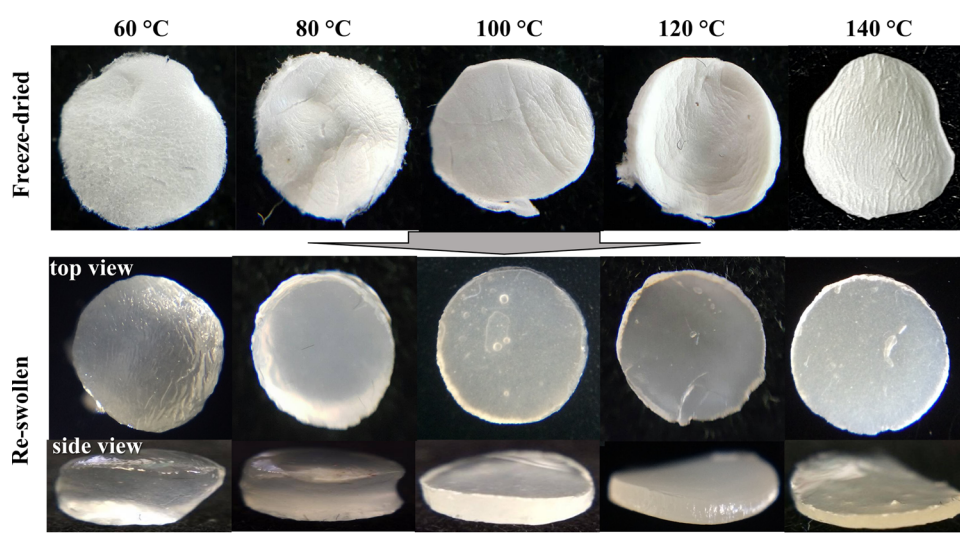


**Figure 3.** Photographs of freeze-dried samples (porous materials) and successive reswollen samples of layered hydrogels, which were prepared by casting the sacran LC solution with a concentration of 0.5% w/v and then cross-linking thermally at 60, 80, 100, 120, and 140 °C. The scale bar is 1 mm.

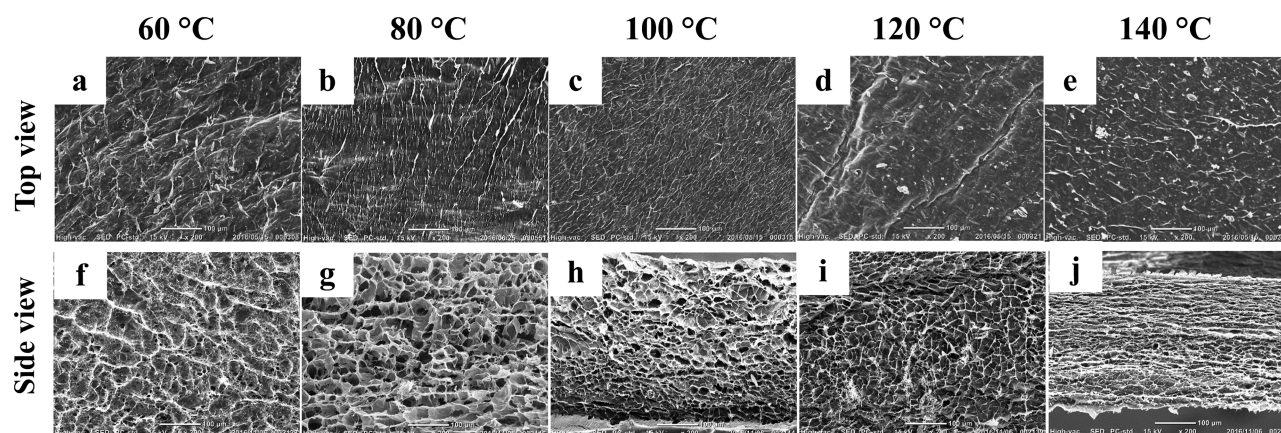


**Figure 4.** SEM images of freeze-dried samples of layered hydrogels, which were prepared by casting the sacran LC solution with a concentration of 0.5% w/v and then thermally cross-linking at 60 (a, f), 80 (b, g), 100 (c, h), 120 (d, i), and 140 °C (e, j). Side views (f–j) reveal pore structure, whereas top views (a–e) reveal no pore structure. The scale bar is 100  $\mu\text{m}$ .

carboxylic and hydroxyl groups, intermolecular hydrogen bonds might be generated by annealing.<sup>36–38</sup> Moreover, it is possible to form ester or ether bonds among these functional groups (Figure S4). This is why the annealing temperature of the sacran sponge affected the gelation behavior. The pores were successfully formed by freeze drying, and the subsequent thermal treatment method but actually the hydrogels did not exhibit appropriate toughness. Such an unexpected result of hydrogel brittleness could be due to randomly directed LC domains, as illustrated in Figure 1a, where the interdomain boundary might induce the brittleness. Moreover, thermal cross-linking of sacran chains beyond the boundaries is probably difficult because the sacran chains are attached in different directions. In summary, simple freeze drying of the sacran solution is not suitable for the production of tough and porous sacran hydrogels. Consequently, our efforts have been devoted to improving the physical properties of porous sacran hydrogels. We developed a method for obtaining tough sacran hydrogels using a solvent-casting method. The toughness was induced by uniaxial orientation of the sacran chains in LC

monodomains formed through fusing small-orientation domains under interfacial effects (Figure 1).<sup>35</sup>

**Preparation of Layered/Porous Hydrogels.** The porous hydrogels with a layered structure were prepared from the sacran LC solution (Figure 1a). The LC solution was dried on a flat substrate, such as plastic, to form a cast film with an in-plane orientation of sacran chains and then the film was thermally cross-linked at 60, 80, 100, 120, and 140 °C (Figure 1b). When the film was immersed in water, hydrogels with a layered structure were formed, which are regarded here as original hydrogels (Figure 1c). The porous hydrogels were prepared by freeze drying to form sponges, which were then reswollen in water (Figure 1e). In frozen state, the sacran network layers were surrounded by ice crystal (Figure 1d). Consequently, pores were formed by passing water vapor to outside of gels in sublimation of ice crystals. Freeze–thawed examples of the original hydrogels were prepared for comparison to those that were freeze-dried. Figures 2 and S5 show representative SEM images of sacran films cast from an LC solution and then annealed at 60 °C (Figure 2a,c) and 140 °C (Figure 2b,d). Regardless of annealing temperatures, the

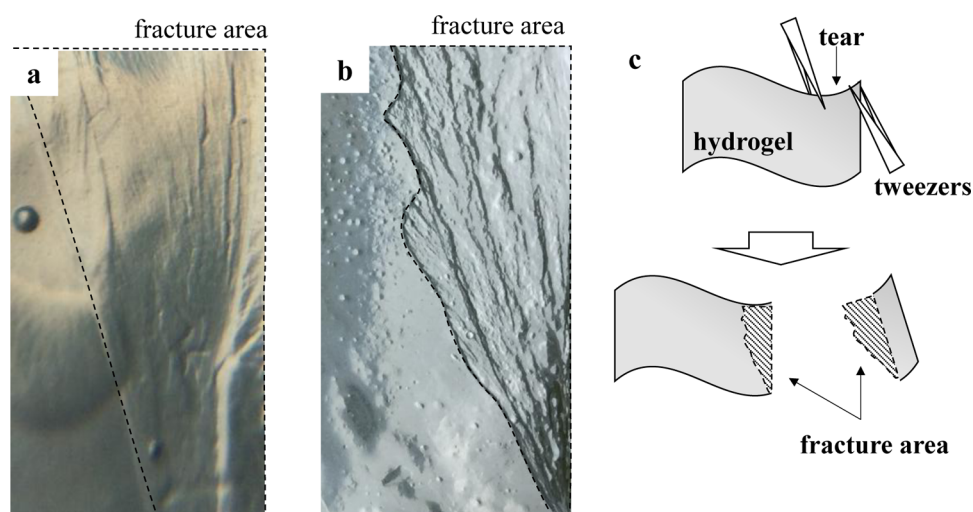


**Figure 5.** Photographs of partially torn samples from the edges of hydrogels derived from the films thermally cross-linked at 60 °C, by (a) freeze-drying and (b) freeze–thawing methods. Illustration (c) shows how to conduct a tear test of hydrogels. Fracture areas are marked by dotted lines. Both photographs show steps in the fracture area of hydrogels suggesting layered structures.

SEM images of the top view of the film show that they are very smooth with no particular structure (Figure S5a,b), whereas those of the side view for cross-sectional samples (Figure 2) show striped lines, which revealed that in-plane orientation of sacran molecules formed layered structures in micrometer scale. In the original hydrogels, in-plane orientation inducing layered structure was confirmed by cross-polarizing optical microscopic images under first-order retardation plate (530 nm) (Figure S6). No distinct difference in the layered structure on these SEM images was observed. From this observation, we confirmed that the layered structure was formed throughout the films. The film was swollen in water and freeze-dried to produce white sponges, whose appearances are shown at the top of Figure 3. The sponges looked denser in the case of the higher thermal-cross-linking temperature, which agrees with the above-mentioned phenomenon using a sacran solution. The hydrogel structures of fluorescein isothiocyanate (FITC)-labeled sacran in the state of Figure 1e were observed by confocal laser scanning micrograph (CLSM), to reveal the porous structures (Figure S7). From the photos, the pore sizes are approximated to  $37 \pm 12$ ,  $26 \pm 5$ ,  $19 \pm 4$ ,  $17 \pm 5$ , and  $13 \pm 3$   $\mu\text{m}$  for hydrogels cross-linked at 60, 80, 100, 120, and 140 °C, respectively. These data also indicated that the network density of precursor hydrogels strongly affected the pore sizes. Differently from the literature,<sup>35</sup> thermal treatment of dried porous film did not remove the pores of the water-swollen hydrogels, presumably owing to the stiffness of rigid sacran chains capable of showing LC phase. Figure 4 shows SEM images of freeze-dried samples of the original hydrogels with layered structures, where the porous pattern can be observed only in the side view, whereas both top and bottom surfaces show some unclear wrinkle-like structures but no pore structures. The porous patterns can be observed in all of the cross sections of these sponges cut by a very sharp surgical knife, revealing the interconnection of pore structures like tunnels. The interconnected pore structures were observed in samples cross-linked at all annealing temperatures. The absence of pores in the top and bottom surfaces is interesting because a simple freeze-drying treatment induced such oriented tunnel structures. The pores were formed by ice sublimation, and the vapor appeared to preferentially vent out of the side faces but

never break the top and bottom surfaces. This phenomenon strongly suggests that the sacran primary layers should be very tough intrinsically owing to strong interchain interactions. At the same time, the wrinkled structures on the top and bottom surfaces were formed on the surface because of the pressure change due to the outflow of water.<sup>39</sup> When the sponges were immersed in deionized water, translucent hydrogels were prepared as shown at the bottom of Figure 3. The hydrogels were somewhat opaque because of the LC phase. As mentioned above, first, freeze-dried samples of sacran LC solutions were annealed but failed to form porous hydrogels having layered structure. Thus, the timing for thermal cross-linking is important to form stable hydrogels. This suggests that sacran molecular chains should be strongly interacted in oriented domains to make thermal cross-linking efficient.

Even after immersion in water, the hydrogels still kept in-plane orientation, which was suggested by the following test: samples were torn from the edges of porous hydrogels by two pairs of tweezers and fracture regions were observed. When they are torn, the hydrogels were not very smoothly fractured to get rough fracture area, whereas regular hydrogels are very easily broken by such a strong twisting stress. Figure 5 shows representative photographs of the fracture area of the hydrogels derived from the films thermally cross-linked at 60 °C. One can see many steps in the fracture areas marked by dotted lines in Figure 5a, strongly suggesting the layered structure formation in hydrogels. The hydrogels produced by a freeze–thawing method, which is widely used to prepare hydrogel-type tissue engineering scaffolds and so on,<sup>40–44</sup> were also prepared for comparison to clarify the freezing effects on hydrogel structures and properties. The freeze–thawed hydrogels also showed steps, suggesting the maintenance of the layered structure (Figure 5b), but had no pores. They are good examples for comparison to the freeze-dried hydrogels.

**Pore Structures.** Figure 4a shows that the pores in the side face observed by SEM seem smaller in the hydrogels prepared from the films cross-linked at higher temperatures. The pore size was estimated from these SEM images and found to range between 10 and 35  $\mu\text{m}$ . The size was plotted against the thermal-cross-linking temperature from 60 to 140 °C to obtain Figure 6a, showing a quantitative tendency of pore-size

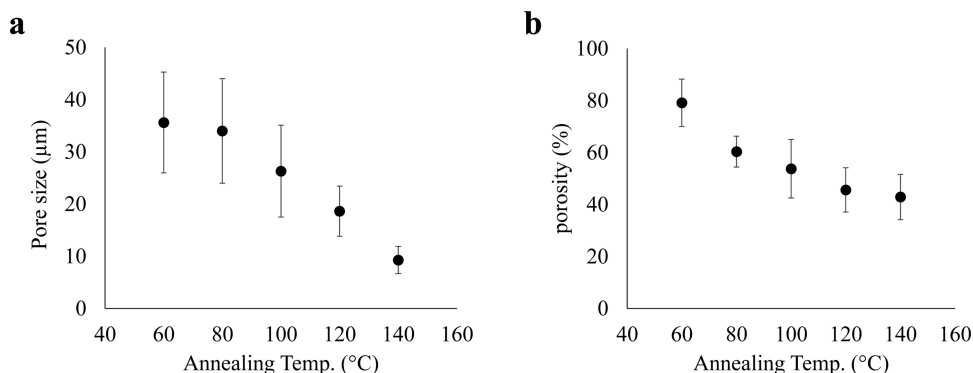


**Figure 6.** Pore size (a) and porosity (b) of freeze-dried samples of layered hydrogels, which were prepared by casting the sacran LC solution with a concentration of 0.5% w/v and then thermally cross-linking at 60, 80, 100, 120, and 140 °C. Pore size (a) was estimated from side views of SEM images (Figure 4f–j), and porosity (b) was evaluated from the amount of tetralin intruding into sample pores.

decrease with increasing thermal-cross-linking temperature, which is well in agreement with the results of CLSM. The sizes determined by SEM in the dry state almost correspond to those by CLSM for high cross-linking temperatures. The tendency corresponds to the shrinking of pores by thermal treatment for freeze-dried sponges, and the layered structure remaining at 140 °C can be easily identified in Figure 4j. We therefore conjecture that annealing the film can enhance intralayer interaction of the sacran chains to make the layers stiff. The water vapor should make pores around the portions where sacran chains interact weakly between layers.

Figure 6b shows the relationship between annealing temperature and porosity, which was measured by taking the volume of voids over the total volume inside xerogels. If freeze-dried sponges were immersed in tetralin, which is not a solvent for sacran chains, the sponges readily absorbed the tetralin. This phenomenon could have occurred due to capillary effects, allowing water to intrude through pores to hydrate the sacran chains. The porosity values of all freeze-dried hydrogels were higher than 40% and were affected by the annealing temperature. The porosity was 79% at an annealing temperature of 60 °C. These results indicate that the pore size and porosity in hydrogels can be controlled by varying the annealing temperature of sacran films. Because pore structures are important for applications such as filters,<sup>3–5</sup> catalyst supports,<sup>6</sup> and tissue engineering scaffolds,<sup>7,8,45</sup> the good controllability is an advantage in these applications. The porosity values are higher than those reported by Nasri-Nasrabadi et al. (25–50%) on a porous composite of starch/cellulose.<sup>46</sup> The porous starch/cellulose was prepared by the combination of film-casting, salt-leaching, and freeze-drying methods. By this method, it is difficult to use big salt particles as a porogen due to brittleness or homogeneity. The results of the method used in the present study were characterized by large and interconnected pores and high porosity.

**Swelling Behaviors.** The effect of annealing temperature on pore structures should have a great influence on swelling behavior. We therefore investigated the swelling degree of porous hydrogels with comparison to nonporous hydrogels prepared by freeze–thawing methods. The swelling degree ( $Q$ , measured in g/g) was determined as the weight ratio of absorbed water to dried polymer, as shown in Tables 1 and S1. The porous hydrogel from the film cross-linked at 60 °C showed a  $Q$  value of 186 g/g, which decreased to 9 g/g at 140 °C. The higher cross-linking temperature yielded smaller pores

**Table 1. Swelling Degrees of Porous and Freeze–Thawed Sacran Hydrogels<sup>a</sup>**

cross-linking temperatures <sup>b</sup> (°C)	porous hydrogels (g/g)	freeze–thawed hydrogels (g/g)
60	186 ± 16 (40 ± 3)	77 ± 3
80	95 ± 6 (38 ± 3)	43 ± 2
100	32 ± 3 (15 ± 1)	23 ± 3
120	16 ± 2 (9 ± 1)	12 ± 1
140	9 ± 0.2 (6 ± 0.1)	9 ± 2

<sup>a</sup>Swelling degrees ( $Q$ ) in distilled water were estimated at room temperature. Values in parentheses refer to matrix-swelling degrees estimated by subtracting pore volumes from entire swelling. <sup>b</sup>Thermal-cross-linking temperatures of layered film as precursors of layered hydrogels.

and a stronger intralayer interaction to disturb the water-molecule absorption into the hydrogels.

We prepared the freeze–thawed hydrogels to examine the freezing effects on hydrogel properties by comparing them to original hydrogels and to examine the drying effects by comparing them to porous hydrogels from freeze-dried sponges. The freeze–thawed samples showed a lower degree of water swelling than porous hydrogels at all thermal-cross-linking temperatures (Table 1), presumably due to the strong effects of interconnected pores on enhancing water absorption through capillary force. On the other hand, the swelling degree of the network matrix of sacran chains was calculated using the data on porosity, and the resulting values are shown in parentheses. These values were lower than those for freeze–thawed hydrogels, suggesting that the drying process also has an effect on decreasing the degree of swelling. For the comparison of freeze–thawed hydrogels with original hydrogels, the swelling degree increased only slightly, indicating that freezing effects are very weak at controlling the degree of swelling. Poly(vinyl alcohol)s (PVA) are well known for showing the physical cross-linking accomplished by the freeze–thawing technique.<sup>47,48</sup> However, sacran chains have more complex structures than PVA that avoids crystallization. Water content ( $A$ ) was also calculated to estimate the network structure quantitatively, which will be described in detail later. In summary, thermal-cross-linking temperature controlled the swelling behavior well in the present method for producing sacran hydrogels.

**Mechanical Properties.** The mechanical properties of swollen hydrogels were measured by stress–strain tests in elongation mode. Generally, compression mode is widely used

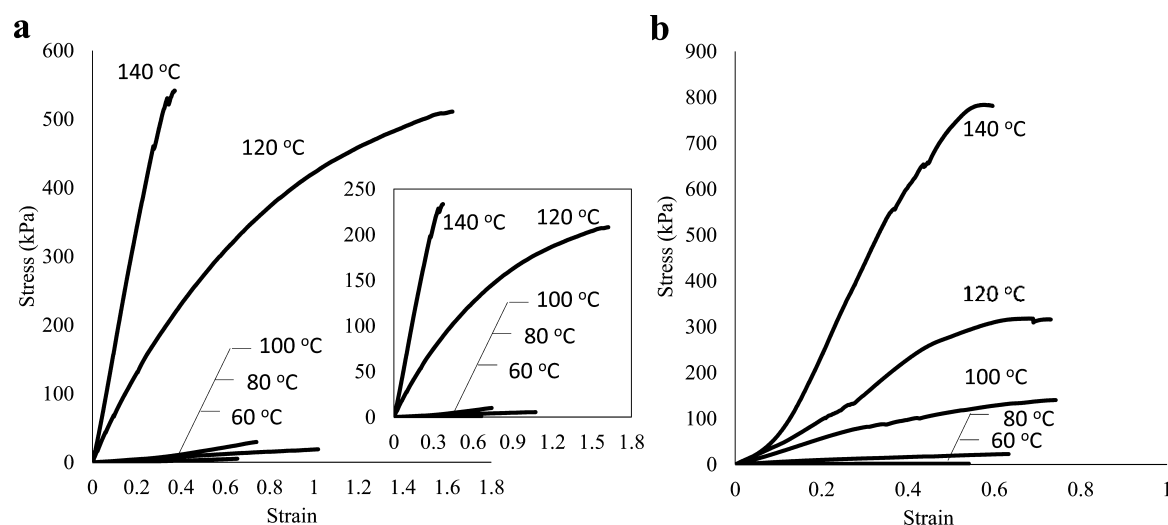


**Figure 7.** Representative stress–strain curves of sacran hydrogels derived from layered films cross-linked thermally at the indicated temperatures. (a) Stress–strain curves of porous hydrogels, where stress values were normalized by matrix areas of water-swollen networks; inset: original stress–strain curves. (b) Freeze–thawed and equilibrated swollen curves.

for hydrogel mechanical test because the elongation mode requires an intrinsic toughness of the samples. Figure 7a shows stress–strain curves of water-swollen sacran networks in porous hydrogels, which were obtained by normalization of the curves for porous hydrogels (inset of Figure 7a) using porosity. The curves show a typical shape, including initial Hookean regions. Elongation tests of freeze–thawed hydrogels were conducted (Figure 7b), and Figure S8 shows the stress–strain curves of original hydrogels. Elastic modulus ( $E$ ), tensile strain at fracture ( $\sigma$ ), elongation at fracture ( $\epsilon$ ), and strain-energy density are summarized in Table 2, whereas the mechanical properties and network analysis of original hydrogels are summarized in Table S2.

$E$  and  $\sigma$  were increased because of the increase in the cross-linking temperature. The increasing cross-linking temperature resulted in proportionally higher  $E$  and  $\sigma$  values of the sacran-layer porous hydrogels, suggesting that the establishment of an increasing cross-linking temperature enlarged the cross-linking point.  $E$  and  $\sigma$  values of porous hydrogels showed an increasing trend from 3 kPa (60 °C) to 585 kPa (140 °C) and from 1 kPa (60 °C) to 210 kPa (140 °C), respectively, by an increase in annealing temperature. On the other hand,  $\epsilon$  values were highest at an annealing temperature of 120 °C. Thermal cross-linking can induce strength and hardness in hydrogels, but too many cross-linking points cause brittleness.  $E$  and  $\sigma$  values of freeze–thawed hydrogels also increased from 5 kPa (60 °C) to 1745 kPa (140 °C) and from 2 kPa (60 °C) to 758 kPa (140 °C), respectively. Porous hydrogels showed 210- and 195-fold increases, whereas those that were freeze–thawed showed 379- and 349-fold increases in  $\sigma$  and  $E$ , respectively. The difference in the rate of increases may be related to no cross-linking inside the pores. Actually,  $\sigma$  and  $E$  values of sacran chain networks in porous hydrogels, which were reestimated using matrix cross-sectional areas by subtracting pore areas (values within parentheses in Table 2), are higher than those of porous hydrogels but lower than those of the freeze–thawed ones, except for the case of 60 °C annealing. The high mechanical strength of freeze–thawed hydrogels may be attributed to interlayer interaction breakage by the pore generation. Strain-energy density, which can be regarded as the measure of toughness in materials science and calculated by the area under

the stress–strain curves, showed a continual increase from 1 kJ/m<sup>3</sup> (60 °C) to 208 kJ/m<sup>3</sup> (140 °C) for freeze–thawed hydrogels, whereas the porous hydrogels showed a maximum strain-energy density of 91 kJ/m<sup>3</sup> at 120 °C, which decreased to 43 kJ/m<sup>3</sup> at 140 °C. This maximum value was caused by the  $\epsilon$ -value tendency. Although the strain-energy densities of porous hydrogels were lower than those of freeze–thawed hydrogels, the values were comparable to those of polymethacrylate-derivative hydrogels<sup>49</sup> applied practically for contact lens and were higher than those of poly(acrylic acid) hydrogels prepared using silica nanoparticle porogens.<sup>50</sup>

Moreover, the porous hydrogel from sacran sponges had a maximum  $E$  value of 585 kPa, which is higher than that for other reported hydrogels derived from dextrin,<sup>51</sup> chitosan/collagen,<sup>52</sup> natural silk protein,<sup>53</sup> hyaluronic acid,<sup>54</sup> and cellulose/alginate,<sup>55</sup> which were prepared by chemical cross-linking. This is owing to the in-plane orientation of the sacran LC structures.

Network structure analyses were performed from  $A$  and  $E$  values. Table 3 summarizes cross-linking density ( $V_e$ ), molecular weight between the cross-linking points ( $M_c$ ), molecular length between the cross-linking points ( $L$ ), and the degree of effective cross-linking ( $X$ ). When the temperature was increased from 60 to 140 °C, the values of  $V_e$  and  $X$  increased 81- and 74-fold, whereas  $M_c$  and  $L$  dropped dramatically by 82-fold for porous hydrogels. Similarly, freeze–thawed hydrogels showed increases in  $V_e$  and  $X$  with an increase in cross-linking temperature, but the rates of increase were 176- and 153-fold higher than those of porous hydrogels, respectively, whereas  $M_c$  and  $L$  decreased 174-fold. It can be seen that freeze–thawed hydrogels had higher  $E$  values than porous hydrogels and their water-swollen sacran networks (in parentheses in the tables) in spite of a higher swelling degree than those of water-swollen sacran networks. As a result,  $V_e$  and  $X$  values of freeze–thawed hydrogels increased sufficiently to induce high toughness over 100 kJ/m<sup>3</sup> at thermal-cross-linking temperatures of 120 and 140 °C. Owing to a layered structure, porous hydrogels retained high toughness, although the strain-energy-density values decreased. In the drying step, the ice was substituted by air to make pore gaps, which broke the interlayer cross-linking; however,

Table 2. Mechanical Properties of Porous and Freeze–Thawed Sacran Hydrogels<sup>a</sup>

cross-linking temperatures <sup>b</sup> (°C)	porous hydrogels			freeze–thawed hydrogels		
	$E^c$ (kPa)	$\sigma^d$ (kPa)	$\epsilon^e$ (mm/mm)	$E^c$ (kPa)	$\sigma^d$ (kPa)	$\epsilon^e$ (mm/mm)
60	3 ± 1 (18 ± 5)	1 ± 0.1 (7 ± 1)	0.60 ± 0.06	5 ± 0.2	2 ± 1	0.65 ± 0.09
80	5 ± 1 (19 ± 3)	5 ± 1 (17 ± 3)	0.94 ± 0.47	46 ± 6	28 ± 9	0.74 ± 0.33
100	21 ± 5 (62 ± 16)	13 ± 3 (38 ± 8)	0.88 ± 0.19	250 ± 37	120 ± 18	0.75 ± 0.02
120	220 ± 410 (540 ± 98)	210 ± 44 (520 ± 110)	1.46 ± 0.32	610 ± 50	330 ± 40	0.68 ± 0.14
140	590 ± 130 (1360 ± 290)	200 ± 30 (470 ± 70)	0.40 ± 0.09	1750 ± 430	760 ± 40	0.52 ± 0.08

<sup>a</sup>Mechanical properties were determined from stress–strain curves recorded at room temperature using a tensiometer in an elongation mode. Values in parentheses are mechanical properties reestimated using matrix cross-sectional areas by subtracting pore areas. <sup>b</sup>Thermal-cross-linking temperatures of layered film as precursors of layered hydrogels. <sup>c</sup> $E$  values refer to elastic modulus. <sup>d</sup> $\sigma$  values refer to tensile strength at fracture. <sup>e</sup> $\epsilon$  values refer to elongation at fracture. <sup>f</sup>Strain-energy-density values were estimated from area surrounded by stress–strain curves.

Table 3. Network Structure Analyses of Freeze-Dried and Freeze–Thawed Sacran Hydrogels

cross-linking temperatures <sup>a</sup> (°C)	porous hydrogels			freeze–thawed hydrogels		
	$V_e^b$ (mol/m <sup>3</sup> )	$M_c^c$ (kg/mol)	$L^d$ (Å)	$V_e^b$ (mol/m <sup>3</sup> )	$M_c^c$ (kg/mol)	$L^d$ (Å)
60	6 ± 2 (25 ± 7)	145 ± 40 (35 ± 10)	6900 ± 1900 (1680 ± 470)	8 ± 1	105 ± 11	5000 ± 520
80	9 ± 2 (24 ± 6)	92 ± 23 (36 ± 9)	4400 ± 1120 (1700 ± 440)	63 ± 11	14 ± 3	650 ± 130
100	26 ± 7 (59 ± 17)	34 ± 8 (15 ± 4)	1610 ± 400 (710 ± 170)	270 ± 31	3 ± 0.4	150 ± 19
120	220 ± 45 (430 ± 90)	4 ± 1 (2 ± 0.4)	190 ± 38 (89 ± 20)	530 ± 72	2 ± 0.2	76 ± 10
140	480 ± 89 (930 ± 170)	2 ± 0.3 (1 ± 0.2)	84 ± 14 (44 ± 7)	1410 ± 350	1 ± 0.1	29 ± 7

<sup>a</sup>Thermal-cross-linking temperatures of layered film as precursors of layered hydrogels. <sup>b</sup> $V_e$  values refer to cross-linking density. <sup>c</sup> $M_c$  values refer to molecular weight between cross-linking points. <sup>d</sup> $L$  values refer to molecular length between cross-linking points. <sup>e</sup> $X$  values refer to degree of cross-linking. Values in parentheses are calculated using elastic moduli and water contents for matrix areas of water-swollen networks with neglecting the amount of water in pores and pore areas.

intralayer cross-linking should be kept to some extent, as clearly illustrated in the SEM image in Figure 4j. As reported by Kováčik, not only cross-linking density but also the pore shape and size also show a significant effect on the mechanical properties of porous materials.<sup>56</sup> In our porous hydrogels of sacran LC chains, the tunnel-like pores along the layers were very effective at keeping high strain-energy density in highly porous hydrogels.

## CONCLUSIONS

Freeze drying of water-swollen layered hydrogels of a supergiant LC polysaccharide, sacran, which are prepared by thermal cross-linking of film cast over a sacran LC solution, forms pores only on the side faces of spongy materials, where layer edges are located but no pores are found on the top and bottom faces, as revealed by SEM. The pore size is decreased from 35 to 10  $\mu\text{m}$  by an increase in temperature for thermal cross-linking from 60 to 140  $^{\circ}\text{C}$  depending on the annealing temperature of the film cast. The anisotropic sponge absorbs an oily solvent, tetralin, although sacran does not dissolve in it, presumably owing to capillary force. From the amount of tetralin absorbed, the porosity of the sacran sponge materials was estimated to range between 40 and 80%, decreasing with an increase in the thermal-cross-linking temperature of the cast films. The anisotropic sponges swell in water to form hydrogels. The swelling degrees are estimated as weight ratios of the water-swollen hydrogel to the dry sponge and range between 9 and 186 g/g, higher than those of the original hydrogels (8–51 g/g), indicating that the porous structures are retained in hydrogels. The swelling degree of the network matrix is calculated to be 6–40 g/g by subtracting the amount of water in pores from the whole swelling degree, which was lower than the nonporous hydrogels prepared by freeze–thawing of the original hydrogels. The swelling degrees of freeze–thawed hydrogels are between those of original hydrogels (from cast films) and those of the network matrix, suggesting that both freezing and successive drying are effective on additional cross-linking of original networks. The porous hydrogels are tough enough to tear at their edges, and many steps appeared around torn parts, suggesting that the layered structures from the layered cast film are maintained. Elastic moduli of the porous hydrogels range from 3 to 585 kPa, whereas tensile strengths at fracture range from 1 to 200 kPa. Moreover, strain-energy density of porous hydrogels cross-linked thermally at 120  $^{\circ}\text{C}$  is high at around 91 kJ/m<sup>3</sup>. The high toughness might be attributed to pores arranging between the layers and not reducing the mechanical toughness when the gels are stretched along the longitudinal direction of the layer.

## MATERIALS AND METHODS

**Materials.** Sacran was dedicated from Green Science Material Inc. (Kumamoto, Japan) and used as received. Tetralin and FITC were purchased from TCI, Japan.

**Hydrogel Preparation.** Hydrogels used here were prepared by the procedure shown in Figure 1. First nonporous sacran hydrogels were prepared as precursors for porous ones by a previously reported procedure.<sup>35</sup> The sacran aqueous solution with a concentration of 0.5% (50 mL) prepared by agitating at 80  $^{\circ}\text{C}$  for 8 h was cast into a polypropylene case (50  $\times$  50  $\times$  50 mm<sup>3</sup>) and dried in an oven at 60  $^{\circ}\text{C}$  for 72 h to form translucent films with a thickness of 44  $\pm$  9  $\mu\text{m}$ . The films were punched into disklike samples with a diameter of 5 mm and

thermally treated at 60, 80, 100, 120, and 140  $^{\circ}\text{C}$ , to cross-link the sacran chains in a dry-film state. When the films were immersed in deionized water at room temperature and kept for 24 h, the translucent self-standing hydrogels were of an almost constant diameter, whereas the thickness was increased.

Next, porous sacran hydrogels were prepared by the following procedure. The precursor hydrogels were frozen by keeping in liquid nitrogen for about 10 min and then drying in a freeze-drying apparatus (EYELA, FDU-1200) for 72 h. We were able to confirm their complete drying because the samples spontaneously attached to the glass wall by electrostatic force. As a result of freeze drying, spongy materials were formed. When the sponges were immersed in deionized water, self-standing hydrogels were recovered.

For comparison, nonporous sacran hydrogels were additionally prepared via the following freezing procedure. If the precursor hydrogels frozen by keeping in liquid nitrogen for about 10 min were thawed by leaving at room temperature for 1 h, the hydrogels were recovered. The obtained hydrogels were immersed in deionized water and kept for 24 h to reach an equilibrium swelling state. The freeze–thawed hydrogels were used for comparison to those that were freeze-dried because the former have a simple layered structure with no pores.

CLSM observation (CLSM, FV1000D, Olympus, excited by 488 nm laser and detected the emission signal at 559 nm) of the hydrogels was made using FITC-labeled sacran, which was prepared as follows. FITC was mixed with dimethyl sulfoxide (DMSO) solution of sacran and then the mixture was stirred at room temperature for 3 days. After DMSO was thoroughly diluted by dialysis with replacing the external pure water repeatedly, the inner solution was poured into acetone to get fibrous samples. The samples were collected and dried in vacuo, to get FITC-labeled sacran. The pore structure was analyzed by checking the dark parts of the images.

**Pore-Size Measurement.** SEM (JEOL, JCM-6000PLUS) was used to investigate the sample structures. The samples were mounted onto metal stubs using carbon tape. The stubs were then coated with gold using a sputter coater machine. ImageJ analysis software was used to determine the averaged pore sizes of 20 randomly selected samples. Three different images of one freeze-dried sample were used for the calculation of mean pore size.

**Porosity Measurement.** Porosity was evaluated using the tetralin displacement method as follows. Freeze-dried samples were cut into 5 mm diameter disklike samples and then immersed in tetralin, which is a slightly viscous solvent with a high boiling point. After keeping the samples for 3 days, the weight was measured by an electronic balance. The porosity was then evaluated by the equation

$$\% \text{porosity} = \frac{(W_s - W_d) / \rho_{\text{tetralin}}}{V_s} \times 100 \quad (1)$$

where  $W_d$  is the dry weight,  $W_s$  is the weight in the swollen state, and  $V_s$  is the total volume of the swollen sample. The density of tetralin,  $\rho_{\text{tetralin}}$ , was 0.97 g/cm<sup>3</sup>. The evaluations were repeated five times and the data were averaged.

**Swelling Properties.** The degrees of swelling were measured by the following method. The weights of dry precursor films or sponges were measured before hydrogel formation. The hydrogels swollen in an equilibrated state were weighed after the water on the sample surfaces was removed by



wiping. The degree of swelling ( $Q$ ) was evaluated by the ratio of the swollen weight ( $W_s$ ) to the dry one ( $W_d$ )

$$Q = \frac{W_s}{W_d} \quad (2)$$

The water content ( $A$ ) of the hydrogels was also evaluated by the following equation

$$A = \frac{W_s - W_d}{W_d} \quad (3)$$

The values of five specimens were averaged.

**Mechanical Properties of the Hydrogels.**<sup>57–59</sup> The mechanical properties of the sacran hydrogels were investigated in an elongation test. The elongation probe was set up on an Instron 3365 machine using a 5 kN load cell with a crosshead speed of 1.0 mm/min. Elastic modulus ( $E$ ) of each sample was calculated using the following neo-Hookean equation applied to unidirectional elongation measurements

$$\tau = \frac{F}{A} = E(\lambda - \lambda^{-2}) \quad (4)$$

where  $\tau$  is the stress,  $F$  is the applied force,  $A$  is the original cross-sectional area of the hydrogels,  $E$  is the elastic modulus, and  $\lambda = h/h_0$ , where  $h$  is the hydrogel length under strain and  $h_0$  is the hydrogel length before elongation. Plotting  $F/A$  versus  $(\lambda - \lambda^{-2})$  resulted in a straight line with a slope of  $E$ , which is the modulus of elasticity of the swelling hydrogel.

The effective cross-linking density ( $V_e$ ) was calculated from the swelling ratio and modulus using the equation

$$V_e = \frac{E\sqrt[3]{Q}}{RT} \quad (5)$$

where  $E$  is the elastic modulus,  $Q$  is the swelling degree,  $R$  is the gas constant, and  $T$  is the absolute temperature of the hydrogels.

The average molecular weight between cross-linking points ( $M_c$ ) was calculated using the cross-linking density, as shown in the following equation

$$M_c = \frac{\rho_p}{V_e} \quad (6)$$

where  $\rho_p$  is the density of the dry polymer (sacran  $\approx 0.83$  g/cm<sup>3</sup>).

The average molecular length between cross-linking points ( $L$ ) was calculated using the molecular weight between the cross-linking points, as shown in the following equation

$$L = \frac{M_c L_0}{M_0} \quad (7)$$

where  $L_0$  is the molecular length of the polymer repeating unit (8.6 Å) and  $M_0$  is the molecular weight of the polymer repeating unit.

The degree of cross-linking ( $X$ ) can be estimated theoretically using  $M_c$ , as given in the following equation

$$X = \frac{M_0}{2M_c} \quad (8)$$

## ■ ASSOCIATED CONTENT

### ■ Supporting Information

The Supporting Information is available free of charge on the ACS Publications website at DOI: 10.1021/acsomega.7b00602.

Chemical structure of sacran, sacran sponge prepared by freeze drying, and information of original hydrogels (PDF)

## ■ AUTHOR INFORMATION

### ■ Corresponding Author

\*E-mail: kaneko@jaist.ac.jp. Tel: +81-761-51-1631. Fax: +81-761-51-1635.

### ■ ORCID

Saranyoo Sornkamnerd: 0000-0002-1929-5406

### ■ Notes

The authors declare no competing financial interest.

## ■ ACKNOWLEDGMENTS

The studies have been financially supported by Grant-in-aid for Challenging Exploratory Research (16K14077) from the Ministry of Education, Culture, Sports, Science, and Technology of Japan.

## ■ REFERENCES

- Zhang, H.; Edgar, D.; Murray, P.; Rak-Raszewska, A.; Glennon Alty, L.; Cooper, A. I. Synthesis of porous microparticles with aligned porosity. *Adv. Funct. Mater.* **2008**, *18*, 222–228.
- Luo, R.; Wu, J.; Dinh, N. D.; Chen, C. H. Gradient Porous Elastic Hydrogels with Shape-Memory Property and Anisotropic Responses for Programmable Locomotion. *Adv. Funct. Mater.* **2015**, *25*, 7272–7279.
- Keckes, J.; Burgert, I.; Frühmann, K.; Müller, M.; Kölln, K.; Hamilton, M.; Burghammer, M.; Roth, S. V.; Stanzl-Tschegg, S.; Fratzl, P. Cell-wall recovery after irreversible deformation of wood. *Nat. Mater.* **2003**, *2*, 810–813.
- Colombo, P. In praise of pores. *Science* **2008**, *322*, 381–383.
- Pyzik, A. J.; Li, C. G. New design of a ceramic filter for diesel emission control applications. *Int. J. Appl. Ceram. Technol.* **2005**, *2*, 440–451.
- Twigg, M. V.; Richardson, J. T. Fundamentals and applications of structured ceramic foam catalysts. *Ind. Eng. Chem. Res.* **2007**, *46*, 4166–4177.
- Hench, L. L.; Polak, J. M. Third-generation biomedical materials. *Science* **2002**, *295*, 1014–1017.
- Hollister, S. J. Porous scaffold design for tissue engineering. *Nat. Mater.* **2005**, *4*, 518–524.
- Mitsumata, T.; Miura, T.; Takahashi, N.; Kawai, M.; Okajima, M. K.; Kaneko, T. Ionic state and chain conformation for aqueous solutions of supergiant cyanobacterial polysaccharide. *Phys. Rev. E: Stat., Nonlinear, Soft Matter Phys.* **2013**, *87*, No. 042607.
- Wathoni, N.; Motoyama, K.; Higashi, T.; Okajima, M.; Kaneko, T.; Arima, H. Enhancing effect of  $\gamma$ -cyclodextrin on wound dressing properties of sacran hydrogel film. *Int. J. Biol. Macromol.* **2017**, *94*, 181–186.
- Wathoni, N.; Motoyama, K.; Higashi, T.; Okajima, M.; Kaneko, T.; Arima, H. Physically crosslinked-sacran hydrogel films for wound dressing application. *Int. J. Biol. Macromol.* **2016**, *89*, 465–470.
- Ngatu, N. R.; Okajima, M. K.; Yokogawa, M.; Hirota, R.; Eitoku, M.; Muzembo, B. A.; Dumavibhat, N.; Takaishi, M.; Sano, S.; Kaneko, T.; Tanaka, T.; Nakamura, H.; Suganuma, N. Anti-inflammatory effects of sacran, a novel polysaccharide from *Aphanthece sacrum*, on 2,4,6-trinitrochlorobenzene-induced allergic dermatitis in vivo. *Ann. Allergy, Asthma, Immunol.* **2012**, *108*, 117–122.
- Okajima, M. K.; le Nguyen, Q. T.; Tateyama, S.; Masuyama, H.; Tanaka, T.; Mitsumata, T.; Kaneko, T. Photoshrinkage in poly-

saccharide gels with trivalent metal ions. *Biomacromolecules* **2012**, *13*, 4158–4163.

(14) Okeyoshi, K.; Okajima, M. K.; Kaneko, T. Milliscale Self-Integration of Megamolecule Biopolymers on a Drying Gas-Aqueous Liquid Crystalline Interface. *Biomacromolecules* **2016**, *17*, 2096–2103.

(15) Kaneti, Y. V.; Tang, J.; Salunkhe, R. R.; Jiang, X.; Yu, A.; Wu, K. C. W.; Yamauchi, Y. Nanoarchitected Design of Porous Materials and Nanocomposites from Metal-Organic Frameworks. *Adv. Mater.* **2017**, *29*, No. 1604898.

(16) Alezi, D.; Belmabkhout, Y.; Suyetin, M.; Bhatt, P. M.; Weseliński, Ł. J.; Solovyeva, V.; Adil, K.; Spanopoulos, I.; Trikalitis, P. N.; Emwas, A. H.; Eddaoudi, M. MOF Crystal Chemistry Paving the Way to Gas Storage Needs: Aluminum-Based MOF for CH<sub>4</sub>, O<sub>2</sub>, and CO<sub>2</sub> Storage. *J. Am. Chem. Soc.* **2015**, *137*, 13308–13318.

(17) Zhao, Y.; Lee, S. Y.; Becknell, N.; Yaghi, O. M.; Angell, C. A. Nanoporous Transparent MOF Glasses with Accessible Internal Surface. *J. Am. Chem. Soc.* **2016**, *138*, 10818–10821.

(18) Rieger, K. A.; Cho, H. J.; Yeung, H. F.; Fan, W.; Schiffman, J. D. Antimicrobial Activity of Silver Ions Released from Zeolites Immobilized on Cellulose Nanofiber Mats. *ACS Appl. Mater. Interfaces* **2016**, *8*, 3032–3040.

(19) Klossner, R. R.; Queen, H. A.; Coughlin, A. J.; Krause, W. E. Correlation of Chitosan's Rheological Properties and Its Ability to Electrospin. *Biomacromolecules* **2008**, *9*, 2947–2953.

(20) Tayi, A. S.; Pashuck, E. T.; Newcomb, C. J.; McClendon, M. T.; Stupp, S. I. Electrospinning Bioactive Supramolecular Polymers from Water. *Biomacromolecules* **2014**, *15*, 1323–1327.

(21) Pol, V. G.; Koren, E.; Zaban, A. Fabrication of Continuous Conducting Gold Wires by Electrospinning. *Chem. Mater.* **2008**, *20*, 3055–3062.

(22) Tang, C.; Saquing, C. D.; Harding, J. R.; Khan, S. A. In Situ Cross-Linking of Electrospun Poly(vinyl alcohol) Nanofibers. *Macromolecules* **2010**, *43*, 630–637.

(23) Dong, Z.; Wu, Y.; Clark, R. L. Thermodynamic Modeling and Investigation of the Formation of Electrospun Collagen Fibers. *Langmuir* **2011**, *27*, 12417–12422.

(24) Colosi, C.; Costantini, M.; Barbetta, A.; Pecci, R.; Bedini, R.; Dentini, M. Morphological Comparison of PVA Scaffolds Obtained by Gas Foaming and Microfluidic Foaming Techniques. *Langmuir* **2013**, *29*, 82–91.

(25) Mannoor, M. S.; Jiang, Z.; James, T.; Kong, Y. L.; Malatesta, K. A.; Soboyejo, W. O.; Verma, N.; Gracias, D. H.; McAlpine, M. C. 3D Printed Bionic Ears. *Nano Lett.* **2013**, *13*, 2634–2639.

(26) Zhu, F.; Cheng, L.; Yin, J.; Wu, Z. L.; Qian, J.; Fu, J.; Zheng, Q. 3D Printing of Ultratough Polyion Complex Hydrogels. *ACS Appl. Mater. Interfaces* **2016**, *8*, 31304–31310.

(27) Bhattacharjee, T.; Gil, C. J.; Marshall, S. L.; Uruena, J. M.; O'Bryan, C. S.; Carstens, M.; Keselowsky, B.; Palmer, G. D.; Ghivizzani, S.; Gibbs, C. P.; Sawyer, W. G.; Angelini, T. E. Liquid-like Solids Support Cells in 3D. *ACS Biomater. Sci. Eng.* **2016**, *2*, 1787–1795.

(28) Lim, K. S.; Schon, B. S.; Mekhileri, N. V.; Brown, G. C. J.; Chia, C. M.; Prabakar, S.; Hooper, G. J.; Woodfield, T. B. F. New Visible-Light Photoinitiating System for Improved Print Fidelity in Gelatin-Based Bioinks. *ACS Biomater. Sci. Eng.* **2016**, *2*, 1752–1762.

(29) Plikk, P.; Mälberg, S.; Albertsson, A. C. Design of Resorbable Porous Tubular Copolyester Scaffolds for Use in Nerve Regeneration. *Biomacromolecules* **2009**, *10*, 1259–1264.

(30) Mecerreyes, D.; Grande, H.; Miguel, O.; Ochoteco, E.; Marcilla, R.; Cantero, I. Porous Polybenzimidazole Membranes Doped with Phosphoric Acid: Highly Proton-Conducting Solid Electrolytes. *Chem. Mater.* **2004**, *16*, 604–607.

(31) Lin-Gibson, S.; Cooper, J. A.; Landis, F. A.; Cicerone, M. T. Systematic Investigation of Porogen Size and Content on Scaffold Morphometric Parameters and Properties. *Biomacromolecules* **2007**, *8*, 1511–1518.

(32) Yang, M.; Wu, J.; Bai, H.; Xie, T.; Zhao, Q.; Wong, T. W. Controlling three-dimensional ice template via two-dimensional surface wetting. *AIChE J.* **2016**, *62*, 4186–4192.

(33) Collins, M. N.; Birkinshaw, C. Investigation of the swelling behavior of crosslinked hyaluronic acid films and hydrogels produced using homogeneous reactions. *J. Appl. Polym. Sci.* **2008**, *109*, 923–931.

(34) Madhally, S. V.; Matthew, H. W. T. Porous chitosan scaffolds for tissue engineering. *Biomaterials* **1999**, *20*, 1133–1142.

(35) Okajima, M. K.; Mishima, R.; Amornwachirabodee, K.; Mitsumata, T.; Okeyoshi, K.; Kaneko, T. Anisotropic swelling in hydrogels formed by cooperatively aligned megamolecules. *RSC Adv.* **2015**, *5*, 86723–86729.

(36) Kanimozhi, K.; Khaleel Basha, S.; Sugantha Kumari, V. Processing and characterization of chitosan/PVA and methylcellulose porous scaffolds for tissue engineering. *Mater. Sci. Eng., C* **2016**, *61*, 484–491.

(37) Li, G.; Zhao, Y.; Zhang, L.; Gao, M.; Kong, Y.; Yang, Y. Preparation of graphene oxide/polyacrylamide composite hydrogel and its effect on Schwann cells attachment and proliferation. *Colloids Surf., B* **2016**, *143*, 547–556.

(38) Wu, J.; Meredith, J. C. Assembly of Chitin Nanofibers into Porous Biomimetic Structures via Freeze Drying. *ACS Macro Lett.* **2014**, *3*, 185–190.

(39) Yang, C. H.; Lin, Y. Y. Surface wrinkles of swelling gels under arbitrary lateral confinements. *Eur. J. Mech.-A/Solids* **2014**, *45*, 90–100.

(40) Mitsumata, T.; Hasegawa, C.; Kawada, H.; Kaneko, T.; Takimoto, J.-i. Swelling and viscoelastic properties of poly(vinyl alcohol) physical gels synthesized using sodium silicate. *React. Funct. Polym.* **2008**, *68*, 133–140.

(41) Lin, C.; He, G.; Dong, C.; Liu, H.; Xiao, G.; Liu, Y. Effect of Oil Phase Transition on Freeze/Thaw-Induced Demulsification of Water-in-Oil Emulsions. *Langmuir* **2008**, *24*, 5291–5298.

(42) Zhao, J.; Bolisetty, S.; Adamcik, J.; Han, J.; Fernández-Ronco, M. P.; Mezzenga, R. Freeze–Thaw Cycling Induced Isotropic–Nematic Coexistence of Amyloid Fibrils Suspensions. *Langmuir* **2016**, *32*, 2492–2499.

(43) Niven, R. K.; Singh, K. Mobilization and Rupture of LNPAL Ganglia during Freeze–Thaw: Two-Dimensional Cell Experiments. *Environ. Sci. Technol.* **2008**, *42*, 5467–5472.

(44) Liu, B.; Mazouchi, A.; Gradinaru, C. C. Trapping Single Molecules in Liposomes: Surface Interactions and Freeze–Thaw Effects. *J. Phys. Chem. B* **2010**, *114*, 15191–15198.

(45) Freed, L. E.; Engelmayr, G. C.; Borenstein, J. T.; Moutos, F. T.; Guilak, F. Advanced Material Strategies for Tissue Engineering Scaffolds. *Adv. Mater.* **2009**, *21*, 3410–3418.

(46) Nasri-Nasrabadi, B.; Mehra, M.; Rafienia, M.; Bonakdar, S.; Behzad, T.; Gavanji, S. Porous starch/cellulose nanofibers composite prepared by salt leaching technique for tissue engineering. *Carbohydr. Polym.* **2014**, *108*, 232–238.

(47) Ricciardi, R.; Auriemma, F.; Gaillet, C.; De Rosa, C.; Lauprêtre, F. Investigation of the Crystallinity of Freeze/Thaw Poly(vinyl alcohol) Hydrogels by Different Techniques. *Macromolecules* **2004**, *37*, 9510–9516.

(48) Ricciardi, R.; Auriemma, F.; De Rosa, C.; Lauprêtre, F. X-ray Diffraction Analysis of Poly(vinyl alcohol) Hydrogels, Obtained by Freezing and Thawing Techniques. *Macromolecules* **2004**, *37*, 1921–1927.

(49) Jackson, A. P. Measurement of the fracture toughness of some contact lens hydrogels. *Biomaterials* **1990**, *11*, 403–407.

(50) Yang, J.; Han, C. R.; Duan, J. F.; Xu, F.; Sun, R. C. In situ grafting silica nanoparticles reinforced nanocomposite hydrogels. *Nanoscale* **2013**, *5*, 10858–10863.

(51) Molinos, M.; Carvalho, V.; Silva, D. M.; Gama, F. M. Development of a hybrid dextrin hydrogel encapsulating dextrin nanogel as protein delivery system. *Biomacromolecules* **2012**, *13*, 517–527.

(52) Martínez, A.; Blanco, M. D.; Davidenko, N.; Cameron, R. E. Tailoring chitosan/collagen scaffolds for tissue engineering: Effect of composition and different crosslinking agents on scaffold properties. *Carbohydr. Polym.* **2015**, *132*, 606–619.

(53) Wang, Z.; Wang, J.; Jin, Y.; Luo, Z.; Yang, W.; Xie, H.; Huang, K.; Wang, L. A Neuroprotective Sericin Hydrogel As an Effective

Neuronal Cell Carrier for the Repair of Ischemic Stroke. *ACS Appl. Mater. Interfaces* **2015**, *7*, 24629–24640.

(54) Collins, M. N.; Birkinshaw, C. Morphology of crosslinked hyaluronic acid porous hydrogels. *J. Appl. Polym. Sci.* **2011**, *120*, 1040–1049.

(55) Kirdponpattara, S.; Khamkeaw, A.; Sanchavanakit, N.; Pavasant, P.; Phisalaphong, M. Structural modification and characterization of bacterial cellulose–alginate composite scaffolds for tissue engineering. *Carbohydr. Polym.* **2015**, *132*, 146–155.

(56) Kováčik, J. Correlation between Young's modulus and porosity in porous materials. *J. Mater. Sci. Lett.* **1999**, *18*, 1007–1010.

(57) Zhu, C.; Bettinger, C. J. Photoreconfigurable Physically Cross-Linked Triblock Copolymer Hydrogels: Photodisintegration Kinetics and Structure–Property Relationships. *Macromolecules* **2015**, *48*, 1563–1572.

(58) Salinas, C. N.; Anseth, K. S. Mixed Mode Thiol–Acrylate Photopolymerizations for the Synthesis of PEG–Peptide Hydrogels. *Macromolecules* **2008**, *41*, 6019–6026.

(59) Baier Leach, J.; Bivens, K. A.; Patrick, C. W., Jr.; Schmidt, C. E. Photocrosslinked hyaluronic acid hydrogels: natural, biodegradable tissue engineering scaffolds. *Biotechnol. Bioeng.* **2003**, *82*, 578–589.